



Published in final edited form as:

*Arch Facial Plast Surg*. 2011 ; 13(5): 305–310. doi:10.1001/archfacial.2011.18.

## Towards Personalized Nasal Surgery Using Computational Fluid Dynamics

John S. Rhee, MD, MPH<sup>1</sup>, Sachin S. Pawar, MD<sup>1</sup>, Guilherme J.M. Garcia, PhD<sup>2</sup>, and Julia S. Kimbell, PhD<sup>3</sup>

<sup>1</sup>Department of Otolaryngology and Communication Sciences, Medical College of Wisconsin, Milwaukee, Wisconsin

<sup>2</sup>Department of Pharmacology, University of North Carolina, Chapel Hill, North Carolina

<sup>3</sup>Department of Otolaryngology/Head and Neck Surgery, University of North Carolina, Chapel Hill, North Carolina

### Abstract

**Objective**—To evaluate whether virtual surgery (VS) performed on 3D nasal airway models can predict post-surgical, biophysical parameters obtained by computational fluid dynamics (CFD).

**Methods**—Pre- and post- surgery CT scans of a patient undergoing septoplasty and right inferior turbinate reduction (ITR) were used to generate 3D models of the nasal airway. Prior to obtaining the post-surgery scan, the pre-surgery model was digitally altered to generate three VS models: 1) right ITR only, 2) septoplasty only, and 3) septoplasty with right ITR. The results of the VS CFD analyses were compared with post-surgical CFD outcome measures including nasal resistance, unilateral airflow allocation, and regional airflow distribution.

**Results**—Post-surgery CFD analysis and all VS models predicted similar reductions in overall nasal resistance, as well as more balanced airflow distribution between sides, primarily in the middle region, when compared with the pre-surgery state. In contrast, virtual ITR alone produced little change in either nasal resistance or regional airflow allocation.

**Conclusions**—We present an innovative approach for assessing functional outcomes of nasal surgery using CFD techniques. This preliminary study suggests that virtual nasal surgery has the potential to be a predictive tool that will enable surgeons to perform personalized nasal surgery using computer simulation techniques. Further investigation involving correlation of patient-reported measures with CFD outcome measures in multiple individuals is underway.

### INTRODUCTION

Surgical management of anatomic nasal airway obstruction is very common. In 1992, nasal septoplasty and turbinate surgery were reported to be the third and eighth most commonly performed surgical procedures by otolaryngologists, respectively (at a rate of 15 procedures per 10,000 insured patients).<sup>1</sup> Additionally, functional septorhinoplasty and nasal valve repair procedures are performed for more complex anatomic deformities. Although a variety

---

**Send correspondence to:** John S. Rhee, MD, MPH, Professor, Department of Otolaryngology and Communication Sciences, Medical College of Wisconsin, 9200 West Wisconsin Avenue, Milwaukee, WI 53226, Tel: 414-805-5585, Fax: 414-805-7890, jrhee@mcw.edu.

Presented at the 2010 American Academy of Facial Plastic and Reconstructive Surgery Annual Meeting, Boston, MA, September 24, 2010.

of surgical techniques and approaches are available to the surgeon, there is no consensus on any given surgical approach or on how to define the success of a given approach.

One of the greatest challenges in addressing nasal airway obstruction (NAO) is the lack of correlation between patient-reported symptoms and objective findings.<sup>2</sup> Determining which patients would benefit from surgery as well as selecting a particular surgical approach is primarily based on the clinical assessment and personal experience of the surgeon. Given the subjective nature of the assessment, it is not surprising that reported surgical failure rates are as high as 25–50%.<sup>3–6</sup> The proposed reasons for this finding are multi-factorial and complex, but include the inability to reliably measure nasal function and airflow as well as inconsistent correlations between patient-reported symptoms with objective testing currently available. Additionally, inappropriate patient selection for surgery or choice of surgical approach may contribute to patient dissatisfaction.<sup>5</sup> Therefore, in order to optimize surgical outcomes, more sophisticated tools are needed that would enable surgeons to better assess the nasal airway, identify patients who would potentially benefit from surgery, and determine the optimal surgical intervention.

The complexity of the nasal airway is well suited to the creation of a computational tool to aid surgeons in the diagnosis and treatment of NAO. With the availability of powerful bioengineering computer-aided design software, anatomically accurate 3D computational models can now be generated from computed tomography (CT) or magnetic resonance imaging (MRI) data. Computational fluid dynamics (CFD) software can be used to analyze these models and calculate various anatomic and physiologic measures including nasal airflow, resistance, air conditioning, and wall shear stress. Furthermore, these 3D computational models can be modified to simulate surgical changes (i.e. “virtual surgery”). CFD tools can then be used to study the effects of these changes on nasal function and potentially predict surgical outcomes.

This paper presents early data from an ongoing four year prospective study designed to investigate the relationships between nasal cavity CFD modeling and patient-reported subjective measures of nasal obstruction. The objective of this initial study was to evaluate the ability of CFD modeling to predict actual surgical outcomes using a virtual nasal surgery computational model. This was accomplished by comparing quantitative CFD parameters (nasal resistance and inspiratory airflow allocation) between an actual post-surgery model and three different virtual surgery models. We hypothesized that virtual surgery CFD results would predict post-surgical CFD results with some variability due to differences in the mechanics of the actual surgical steps and the way these steps were translated to the computer model and due to possible random effects of post-surgical healing.

## METHODS

### Patient Recruitment

Patients are being recruited from the Medical College of Wisconsin (MCW) Otolaryngology clinic as part of our larger 4-year prospective study. Inclusion criteria include age 15 years or older and having a clinical diagnosis of a non-reversible, surgically-treatable cause of nasal obstruction (deviated septum, turbinate hypertrophy resistant to medical treatment, or lateral wall collapse). The research protocol was approved by the MCW institutional review board (IRB). The patient presented in this paper is a 30 year old, 86.4-kg female who presented with complaints of nasal airway obstruction and had significant leftward septal deviation with right inferior turbinate hypertrophy.

## Patient Treatment

Modified contiguous computed tomography (CT) scans in the axial plane of the entire nasal cavity and external nasal soft tissue were performed pre-operatively (0.625 mm increments, 0.313 mm resolution) and approximately 6 months post-operatively (0.600 mm increments, 0.313 mm resolution). The decision for the surgical procedure to be performed was made by the surgeon (JR) based on clinical presentation and the standard of medical care. In this case, the patient underwent septoplasty using standard septoplasty techniques and right inferior turbinate reduction. The anterior one-half of the inferior turbinate was debulked by performing submucosal resection of the bone and removal of the submucosal tissue with sharp dissection. No thermal or ablative techniques were used. Post-surgical care was performed in the usual manner following nasal surgery with an uneventful post-operative course.

## Computational Fluid Dynamics Workflow

Our CFD simulation workflow is illustrated in Figure 1. The pre- and post-surgery computer models were created using the pre- and post-surgery CT scan image data, respectively, and the image analysis software Mimics™ 13.1 (Materialise, Plymouth, MI). In addition, the pre-surgery model was digitally altered using Mimics™ to generate three virtual surgery models for analysis: 1) right inferior turbinate reduction only, 2) septoplasty only, and 3) septoplasty with right inferior turbinate reduction (Figure 2). The goal of virtual surgery was to alter the pre-surgical nasal anatomy to reproduce the anticipated surgical changes. Three-dimensional reconstructions of the nasal septum are shown in Figure 3 and illustrate the virtual surgery and actual post-surgery areas of anatomic change. As per the carefully conceived IRB protocol, the virtual surgery models were created after the actual surgery was performed so that surgical decision-making would not be influenced before the ability of CFD to predict patient outcomes has been assessed. Virtual surgery was performed on the pre-surgery model by the surgeon (JR) within 24 hours after the actual surgery to minimize recall bias.

To solve the equations that govern fluid flow, each 3D nasal model must be divided into a large number of small cells where air velocity and pressure can be defined. This was accomplished by creating a mesh with approximately 4 million tetrahedral cells using ICEM-CFD™ (ANSYS, Inc., Canonsburg, PA). Steady-state inspiratory airflow simulations were conducted using Fluent 12.0 (ANSYS, Inc., Lebanon, NH) for airflow rates corresponding to normal resting breathing. The following boundary conditions were used in Fluent to determine the airflow field: (1) a "wall" condition (zero velocity, stationary wall assumed) at the airway walls, (2) a "pressure-inlet" condition at the nostrils with gauge pressure set to 0, and (3) a "pressure-outlet" condition at the outlet with gauge pressure set to a negative value in Pascals that generated the target steady-state flow rate of 15.7 L/min. This flow rate represents an estimate of twice the patient's minute volume (amount of air exhaled in 1 min) based on allometric scaling by body weight.<sup>7</sup> Additional details on the differential equations, computational algorithms, and air physical properties used can be found in previous publications by our group.<sup>8</sup> Figures, printouts, diagrams and other visualizations of CFD model results were made using the visualization software package Fieldview™ (Intelligent Light, Lyndhurst, NJ) as well as the visualization capabilities within Fluent™.

## Outcome Measures

CFD calculated outcome measures included nasal resistance, airflow allocation, and regional airflow distribution within the nasal cavity. Nasal resistance was calculated as  $\Delta p/Q$ , where  $\Delta p$  is the pressure difference in Pascals (Pa) between the nostrils and posterior nose and  $Q$  is the flow rate in milliliters per second (ml/s). For consistency among models and CT scans,

the posterior nose where pressure was measured for calculating nasal resistance was defined as the posterior end of the nasal septum. Airflow allocation measured the percentage of total airflow passing through the left and right nasal cavities. Regional airflow distribution was analyzed through visualization of major inspiratory streamlines and quantified by allocation of volumetric flow to dorsal, middle, and ventral portions of a mid-turbinate coronal cross-section, as described by Subramaniam and colleagues.<sup>9</sup>

## RESULTS

### Nasal Resistance

Pre-surgery, overall nasal resistance was 0.060 Pa/(ml/s) and unilateral right and left nasal resistances were 0.096 Pa/(ml/s) and 0.160 Pa/(ml/s), respectively (Figure 4). Virtual septoplasty with right ITR resulted in a reduction of the overall nasal resistance to 0.046 Pa/(ml/s) while the actual surgery resulted in a reduction of the overall nasal resistance to 0.039 Pa/(ml/s). Virtual septoplasty alone reduced overall nasal resistance to 0.047 Pa/(ml/s) and right ITR alone did not affect the overall nasal resistance.

Both virtual and actual surgery resulted in decreases in unilateral nasal resistances, however, the effect was more pronounced on the patient's left side which was affected by the septal deviation. Virtual septoplasty with ITR resulted in a left-sided nasal resistance of 0.098 Pa/(ml/s) and actual post-surgery left-sided nasal resistance was 0.072 Pa/(ml/s). Virtual septoplasty alone, with a left-sided nasal resistance of 0.098 Pa/(ml/sec), accounted for almost all of the drop in resistance on that side.

### Airflow Allocation

The pre-surgery CFD model estimated that 61.3% of the total airflow passed through the right side while 38.7% passed through the left. The post-surgery and virtual surgery models predicted a more balanced airflow distribution between the two sides (Figure 5). The virtual septoplasty with ITR model and the septoplasty only model resulted in a very similar distribution. In contrast, the ITR only model did not alter the airflow allocation between sides to a great degree with 61.7% of the airflow passing through the right and 38.3% through the left. The actual post-surgery CFD model resulted in an airflow allocation slightly favoring the left side when compared to the CFD predicted results for the virtual surgery models. Differences in airflow allocation between the actual post-surgery and virtual surgery models may have been due to the nasal cycle, since pre- and post-surgery CT imaging suggested that the patient was cycling on opposite sides when the two CT scans were taken.

### Regional Airflow Distribution

In the pre-surgery CFD model, the majority of the airflow passed through the right middle region. In contrast, the post-surgical model showed more balanced airflow through the right and left sides with increased airflow through the left middle region and minimal dorsal airflow (Figure 6). The two virtual surgery models that included septoplasty showed a similar increase in left middle airflow and slightly decreased right middle airflow, although these changes were less in magnitude than the actual post-surgical results. The virtual ITR only model shows negligible change in regional airflow allocation when compared to the pre-surgery model.

## COMMENT

As part of an ongoing 4-year prospective study, we have presented a case report of virtual nasal surgery and CFD techniques applied to computational models generated from a patient

with nasal airway obstruction secondary to septal deviation and inferior turbinate hypertrophy. A complete comparison between the pre-surgery and actual post-surgery CFD results and correlation with patient-reported measures will be reported in a future publication. The focus of this study was to establish the potential application of virtual nasal surgery and determine the predictive utility of virtual surgery CFD modeling with respect to actual post-surgical outcomes.

To date, relatively little research has been published in the area of virtual nasal surgery. Although no other study has compared virtual nasal surgery CFD results with actual post-surgical outcomes, CFD techniques have been increasingly used to study various simulated alterations of the human nasal airway over the past decade. Some authors have described simulated nasal surgery procedures using computerized models, typically by using CT scans from subjects with normal nasal anatomy which are then altered to create a “virtual surgery” nasal model with the appropriate modifications.<sup>10-12</sup> Others have altered computer models with abnormal anatomy to assess post-operative effects but these have not been compared with actual post-surgical results, therefore limiting the generalizability of these results.<sup>13</sup>

Wexler et. al. investigated the changes in unilateral nasal airflow by modeling the circumferential removal of 2 mm of soft tissue along the left inferior turbinate in a computational model generated from a healthy subject without nasal complaints.<sup>10</sup> Another group used imaging from a cadaver with septal deviation and concha bullosa to generate a computational model<sup>13</sup>. These authors simulated a virtual septoplasty and partial lateral turbinectomy and compared CFD calculated airflow and nasal resistance results between the pre- and post- virtual surgery models. In addition to studying nasal airflow patterns, CFD has been used to investigate nasal air conditioning following simulated unilateral resection of the inferior and middle turbinates.<sup>11</sup> Garcia et. al. used 3D software tools on a healthy nose model to create septal deviations in various locations and applied CFD techniques to study the effects on nasal resistance.<sup>14</sup>

Overall, the virtual surgery results are promising and demonstrate the potential of CFD techniques to predict post-surgical outcomes. CFD calculations of overall nasal resistance for the combined virtual septoplasty with ITR model correlated well with the actual post-surgery calculations. Of the three virtual surgery models, the virtual septoplasty with ITR model predicted the lowest overall nasal resistance. Interestingly, results from the various virtual surgery combinations suggest that inferior turbinate reduction may have contributed very little to the reduction of overall nasal resistance in this patient, for whom septal deviation was likely the major contributing factor to nasal resistance. Prior studies, such as that done by Wexler et. al. have supported a decrease in nasal resistance following inferior turbinate reduction<sup>10</sup>, however, this was based on a unilateral analysis only, conducted in a normal airway. In the present study, unilateral nasal resistance also decreased in the virtual surgery and actual post-surgery models.

Airflow allocation results illustrate the improved balance of airflow between the left and right sides compared to pre-surgery. Virtual septoplasty with and without ITR demonstrated similar changes in allocation between sides while the virtual ITR only model showed no difference compared to pre-surgery. This seems to predict that right ITR alone has a negligible impact on airflow allocation between the left and right sides of the nose. This analysis suggests that septoplasty alone could achieve improved airflow allocation without the need for ITR for this patient.

Regional airflow distribution results from the virtual surgery models also showed reasonable correlation with the post-surgery results and allow for more detailed understanding of airflow changes within the nasal cavity as a result of surgery. Here, the general trends

reported on Figure 6 are likely more indicative of the anticipated surgical outcome than the absolute numbers obtained by CFD simulations.

Pre-surgery analysis shows that airflow was restricted in the left middle region due to the large leftward septal deviation. Subsequent virtual septoplasty with and without ITR and the final post-surgery model show noticeable improvement in left middle region airflow with concomitant decrease in right middle airflow to yield a more balanced flow. Again in this analysis, virtual right ITR did not dramatically change regional airflow distribution, suggesting minimal impact from this procedure.

If this type of modeling were utilized in a pre-surgery planning situation, the virtual surgery models suggest that right inferior turbinate reduction, using this particular surgical technique, may have negligible impact on the improvement of symptoms in this particular patient. Compensatory turbinate hypertrophy in the setting of nasal septal deviation is thought to protect the more patent nasal passage from the drying and crusting effects of increased airflow.<sup>15</sup> Histologic analysis of the hypertrophied inferior turbinate has shown that enlargement of the bony layer contributes to 75% of the enlargement of the turbinate as compared to the mucosal layer.<sup>15</sup> The decision to perform turbinate reduction is typically based on the surgeon's clinical judgment and the exact method may vary from surgeon to surgeon. Studies looking at outcomes of turbinate reduction combined with septoplasty have shown variable results and there is no consensus at this time.<sup>6, 16-18</sup> The use of CFD modeling for surgical planning could help determine which patients may benefit from inferior turbinate reduction in the setting of septal deviation. In this particular patient case, the use of pre-surgical CFD planning may have changed the decision to perform ITR using this particular surgical technique, since simulations would have predicted little impact on nasal resistance.

While CFD applications for nasal surgery are certainly promising, there are several inherent limitations in the current state of this technology. CFD modeling techniques rely on several assumptions to simplify the computational process. These include the use of a fixed wall model which cannot account for compliance of the nasal soft tissues in the presence of negative pressure. Additionally, these models assume that complete airflow occurs through the nose only, when in reality patients with varying degrees of nasal airway obstruction will breathe through the mouth, potentially altering the true airflow characteristics in the nose. Another modeling challenge is that each computational model represents the nasal anatomy at a specific point in time. While major structural features will generally be preserved across models, the dynamic nature of the nasal mucosa (i.e. nasal cycling) can vary between models of the same patient and potentially influence direct comparisons. This has the potential to become problematic when applying CFD techniques to the relatively narrow nasal passages, where only a few millimeters of mucosal swelling can result in significant airflow changes. Additionally, although virtual surgery can be done on a static model, the unpredictable and dynamic nature of patient healing can ultimately limit the predictive capability of the model. In addition, important practical considerations include the fact that while CFD software applications have become more widely available and accessible, they remain costly and are often cumbersome to use. Also, the workflow to create computational models and run various simulations is also very time consuming and requires a level of technical expertise that is not available to most surgeons.

As we look to the future, the hope is that this technology can be employed for more routine day-to-day use in the armamentarium of Otolaryngologists and facial plastic surgeons. At this point in time, CFD technology is truly translational in nature and will require further research and development to reach its full potential for future applications. In the meantime, the collection of normative CFD models that is accruing in the literature will be important



for comparison purposes and could be used to help set normal ranges for calculated CFD parameters. We envision a future where a virtual nasal surgery software application using a simplified user interface could be coupled with a sophisticated computational component that is largely transparent to the end-user surgeon. This would allow for the rapid creation of computational models “on-the-fly” using readily available CT imaging data. Using these models, the surgeon could perform an in-office CFD analysis of the patient’s nasal airway and simulate various surgical approaches or maneuvers to create a personalized surgical plan for each patient that would provide the best surgical outcome.

## Acknowledgments

**Funding/Support:** This research was funded in part by grant 1R01EB009557-01 from the National Institutes of Health/National Institute of Biomedical Imaging and Bioengineering.

## REFERENCES

1. Manoukian PD, Wyatt JR, Leopold DA, Bass EB. Recent trends in utilization of procedures in otolaryngology-head and neck surgery. *Laryngoscope*. 1997; 107:472–477. [PubMed: 9111376]
2. Rhee JS. Measuring outcomes in nasal surgery: Realities and possibilities. *Arch Facial Plast Surg*. 2009; 11:416–419. [PubMed: 19917906]
3. Singh A, Patel N, Kenyon G, Donaldson G. Is there objective evidence that septal surgery improves nasal airflow? *J Laryngol Otol*. 2006; 120:916–920. [PubMed: 17040608]
4. Andre RF, D'Souza AR, Kunst HP, Vuyk HD. Sub-alar batten grafts as treatment for nasal valve incompetence; description of technique and functional evaluation. *Rhinology*. 2006; 44:118–122. [PubMed: 16792170]
5. Dinis PB, Haider H. Septoplasty: Long-term evaluation of results. *Am J Otolaryngol*. 2002; 23:85–90. [PubMed: 11893975]
6. Illum P. Septoplasty and compensatory inferior turbinate hypertrophy: Long-term results after randomized turbinoplasty. *Eur Arch Otorhinolaryngol*. 1997; 254(Suppl 1):S89–S92. [PubMed: 9065637]
7. Garcia GJ, Schroeter JD, Segal RA, Stanek J, Foureman GL, Kimbell JS. Dosimetry of nasal uptake of water-soluble and reactive gases: A first study of interhuman variability. *Inhal Toxicol*. 2009; 21:607–618. [PubMed: 19459775]
8. Garcia GJM, Bailie N, Martins DA, Kimbell JS. Atrophic rhinitis: A CFD study of air conditioning in the nasal cavity. *J Appl Physiol*. 2007; 103:1082–1092. [PubMed: 17569762]
9. Subramaniam RP. Computational fluid dynamics simulations of inspiratory airflow in the human nose and nasopharynx. *Inhal Toxicol*. 1998; 10:91–120.
10. Wexler D, Segal R, Kimbell J. Aerodynamic effects of inferior turbinate reduction: Computational fluid dynamics simulation. *Arch Otolaryngol Head Neck*. 2005; 131:1102–1107.
11. Lindemann J, Keck T, Wiesmiller KM, Rettinger G, Brambs H, Pless D. Numerical simulation of intranasal air flow and temperature after resection of the turbinates. *Rhinology*. 2005; 43:24–28. [PubMed: 15844498]
12. Kim S, Chung S. An investigation on airflow in disordered nasal cavity and its corrected models by tomographic PIV. *Measurement Science and Technology*. 2004
13. Ozlugedik S, Nakiboglu G, Sert C, et al. Numerical study of the aerodynamic effects of septoplasty and partial lateral turbinectomy. *Laryngoscope*. 2008; 118:330–334. [PubMed: 18030167]
14. Garcia GJM, Rhee JS, Senior BA, Kimbell JS. Septal deviation and nasal resistance: An investigation using virtual surgery and computational fluid dynamics. *Am J Rhinol Allergy*. 2010; 24:e46–e53. [PubMed: 20109325]
15. Berger G, Hammel I, Berger R, Avraham S, Ophir D. Histopathology of the inferior turbinate with compensatory hypertrophy in patients with deviated nasal septum. *Laryngoscope*. 2000; 110:2100–2105. [PubMed: 11129029]
16. Jun BC, Kim SW, Kim SW, Cho JH, Park YJ, Yoon HR. Is turbinate surgery necessary when performing a septoplasty? *Eur Arch Otorhinolaryngol*. 2009; 266:975–980. [PubMed: 19002479]

17. Kim DH, Park HY, Kim HS, et al. Effect of septoplasty on inferior turbinate hypertrophy. *Arch Otolaryngol Head Neck Surg.* 2008; 134:419–423. [PubMed: 18427009]
18. Nunez DA, Bradley PJ. A randomised clinical trial of turbinectomy for compensatory turbinate hypertrophy in patients with anterior septal deviations. *Clin Otolaryngol Allied Sci.* 2000; 25:495–498. [PubMed: 11122287]



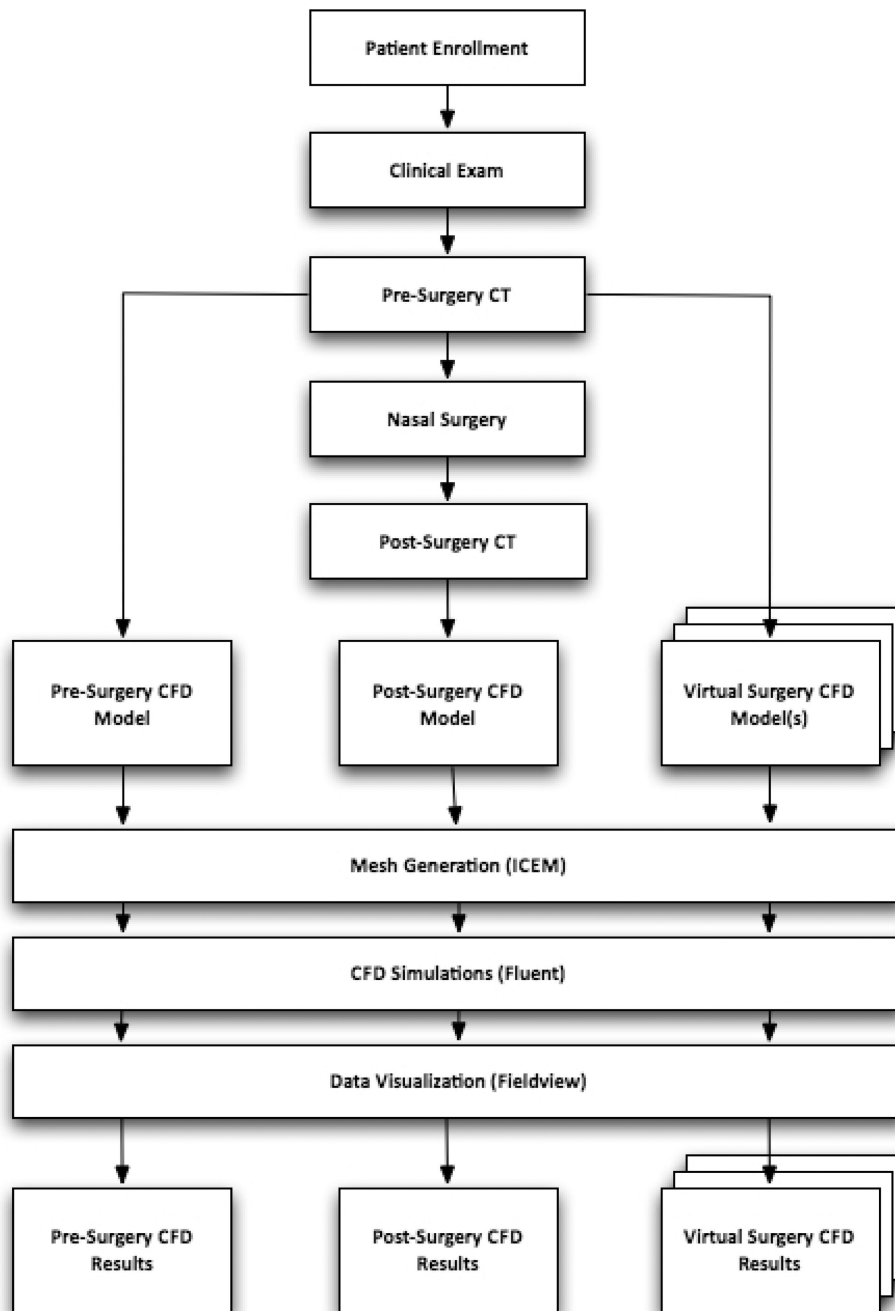


**FIGURE 1.** Diagram of CFD workflow used to generate the various computational models.

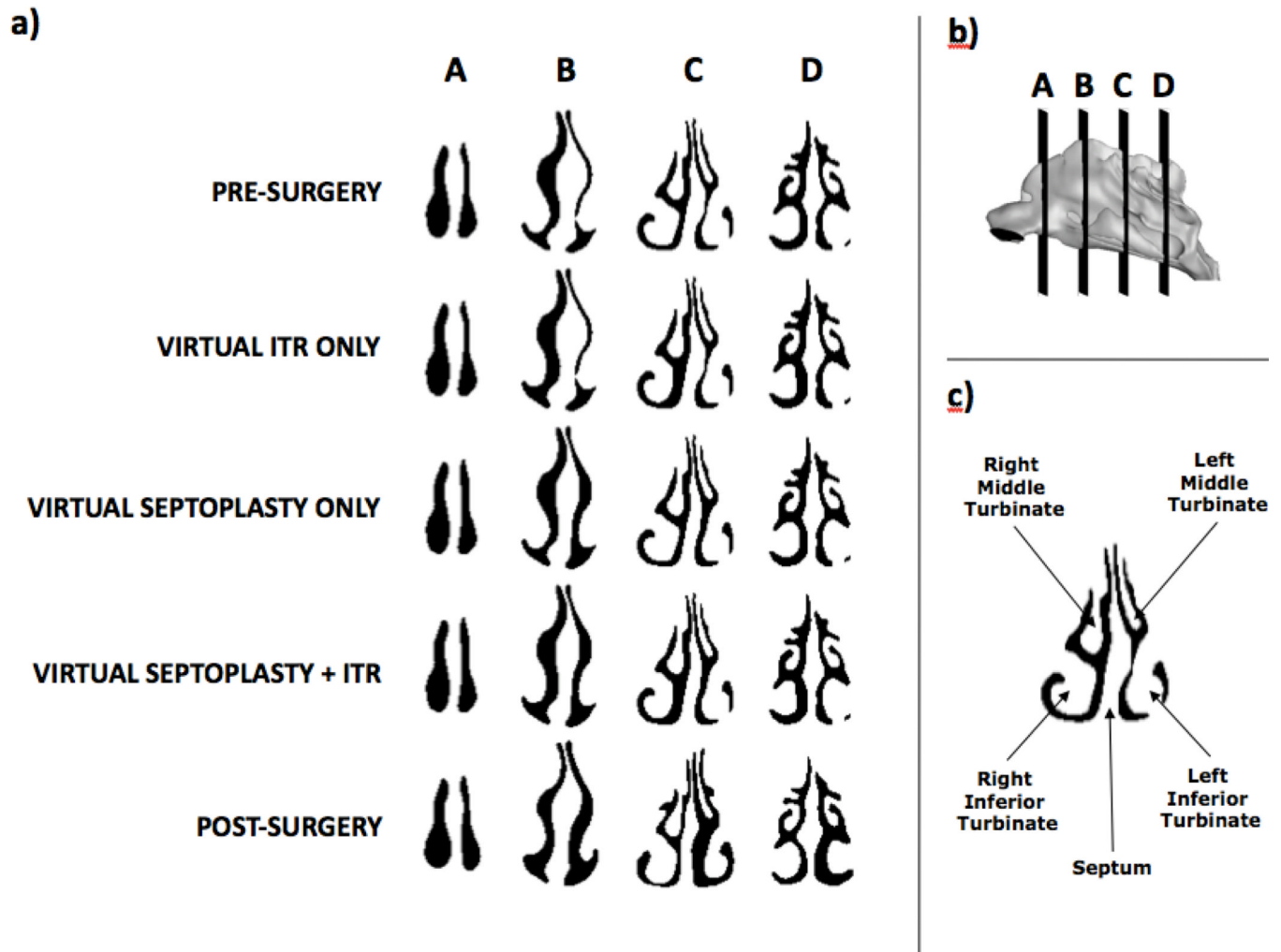


**FIGURE 2.**

(a) Coronal cross sections at four locations (A, B, C, D) illustrating the anatomic differences among the computer models. (b) Para-sagittal 3D nasal reconstruction showing location of coronal planes illustrated in 2a. (c) Representative coronal cross-section identifying location of the inferior turbinates, middle turbinates, and septum.

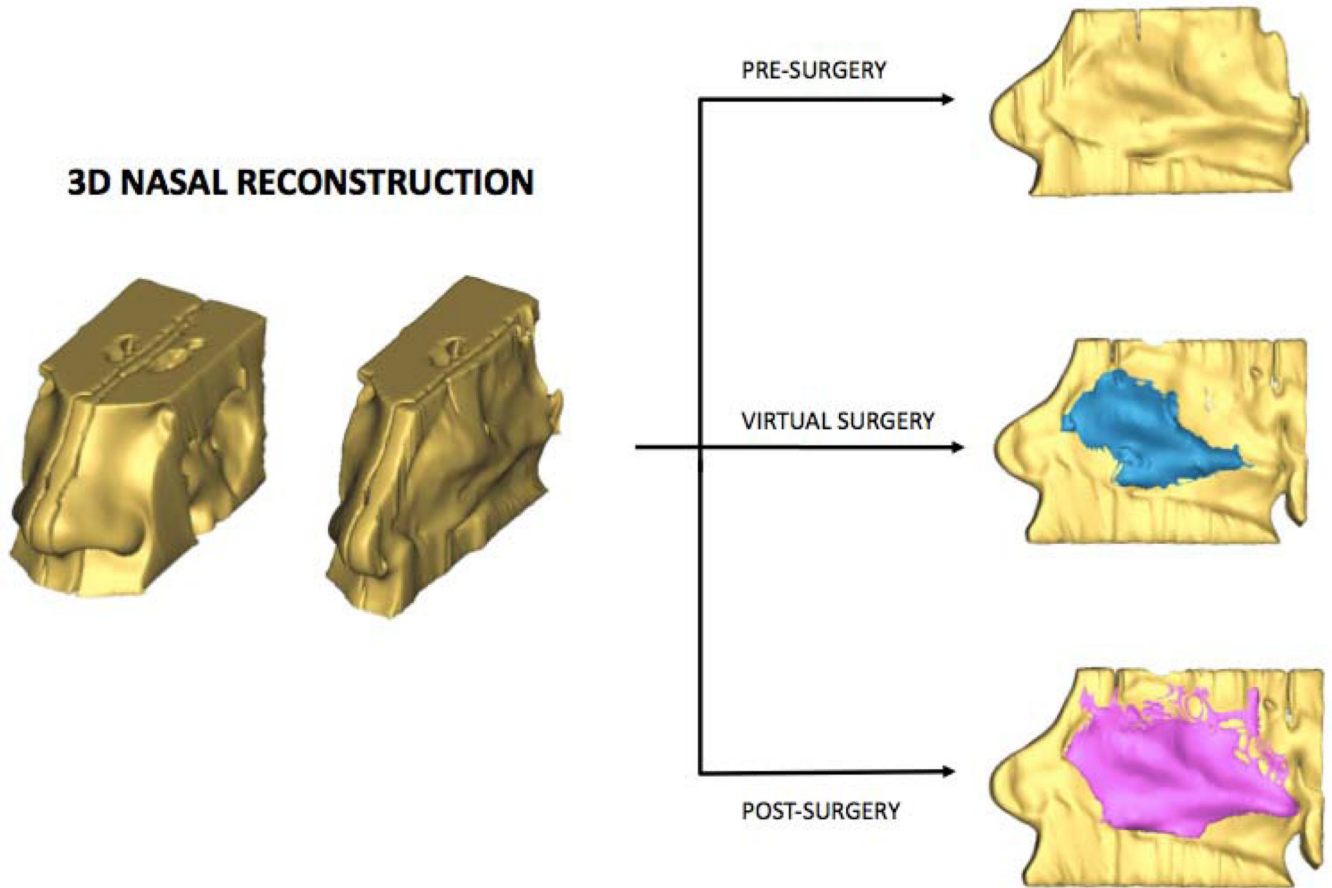


**FIGURE 3.** Three-dimensional nasal reconstructions and left sagittal views of the nasal septum. Colored regions indicate the area of the septum modified in the virtual surgery and post-surgery models.

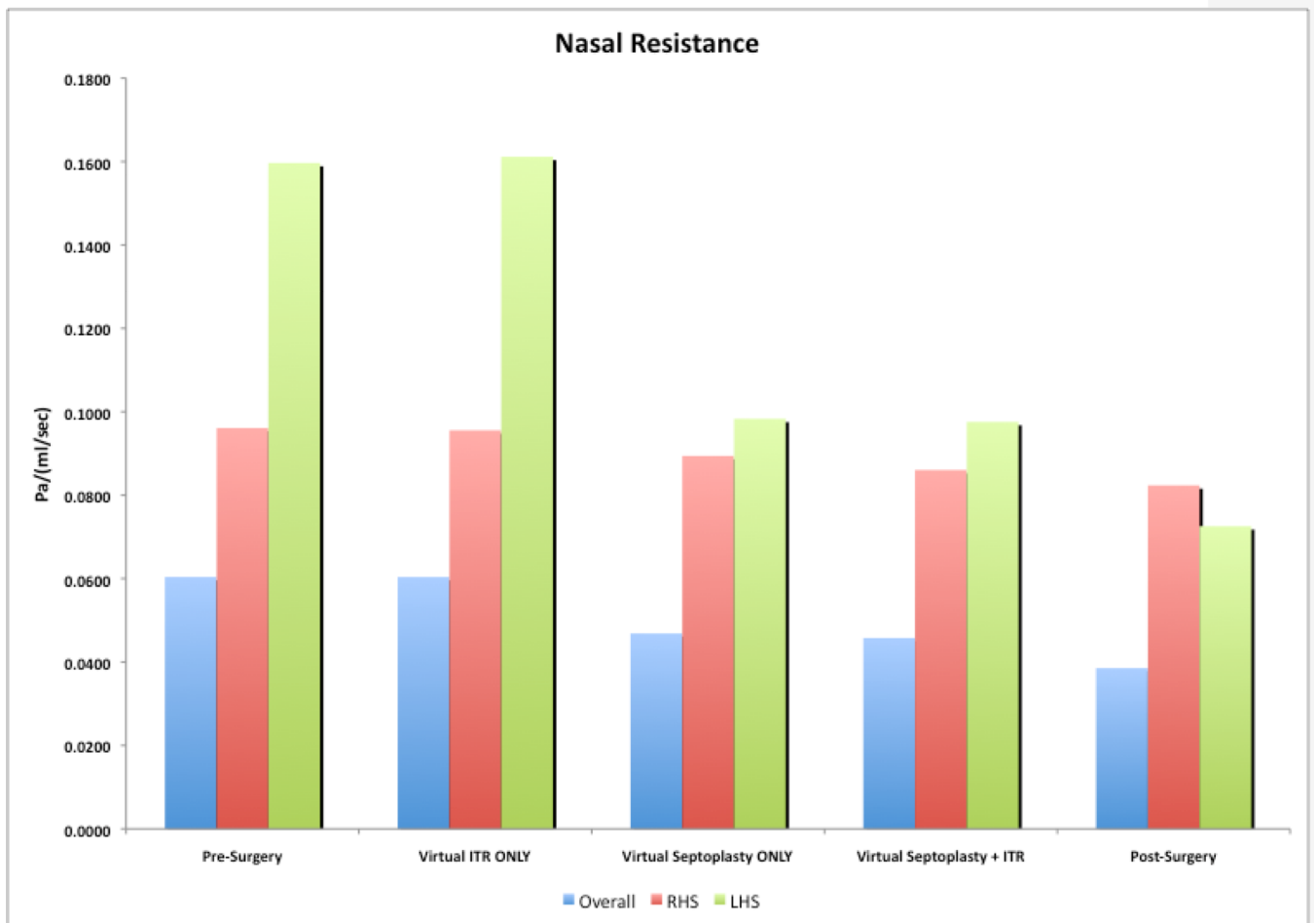


**FIGURE 4.** Overall, right hand side (RHS), and left hand side (LHS) nasal resistance values calculated using CFD.

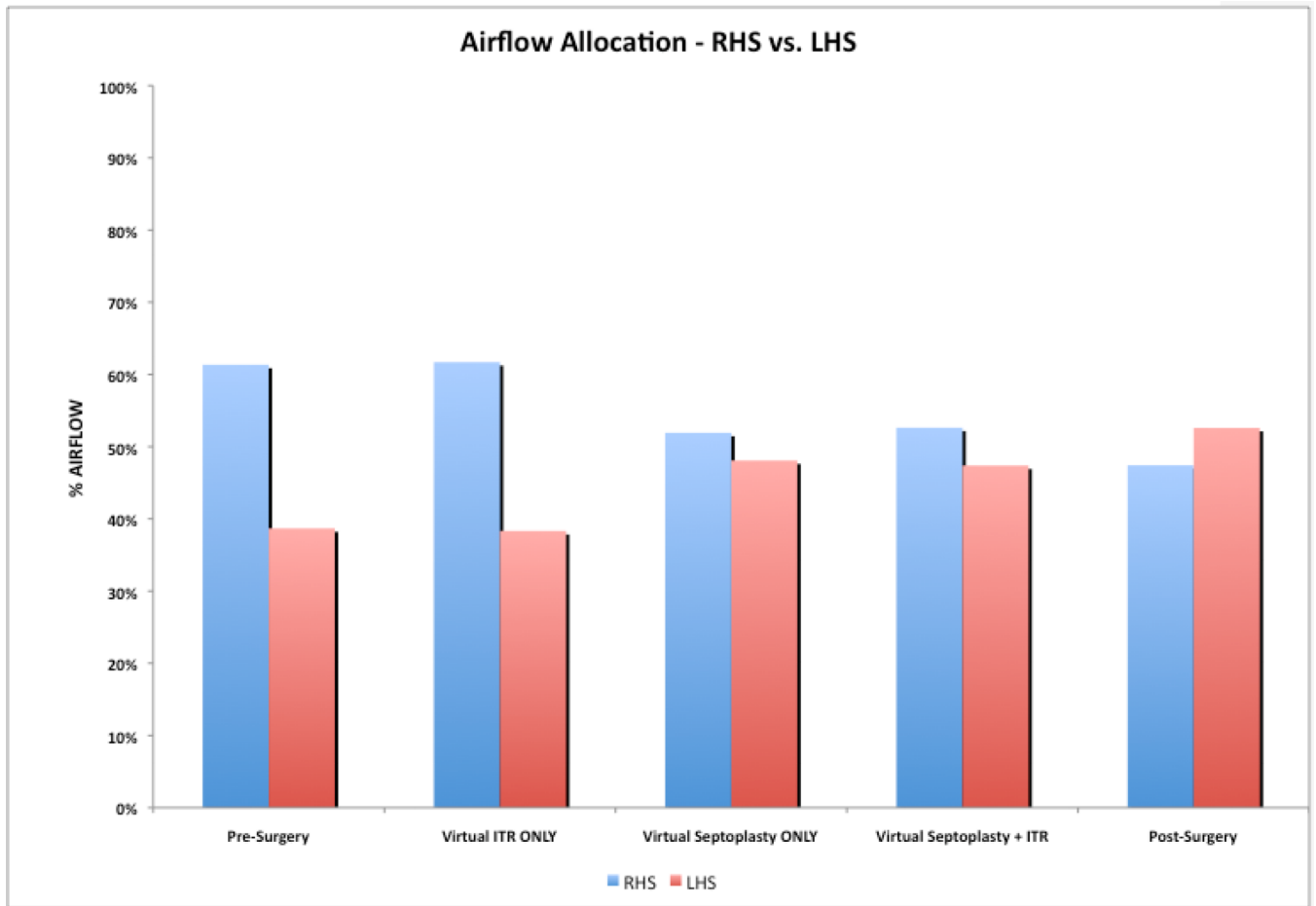


**FIGURE 5.** CFD-calculated airflow allocation between the right hand side (RHS) and left hand side (LHS) of the nose.

## Regional Airflow Distribution

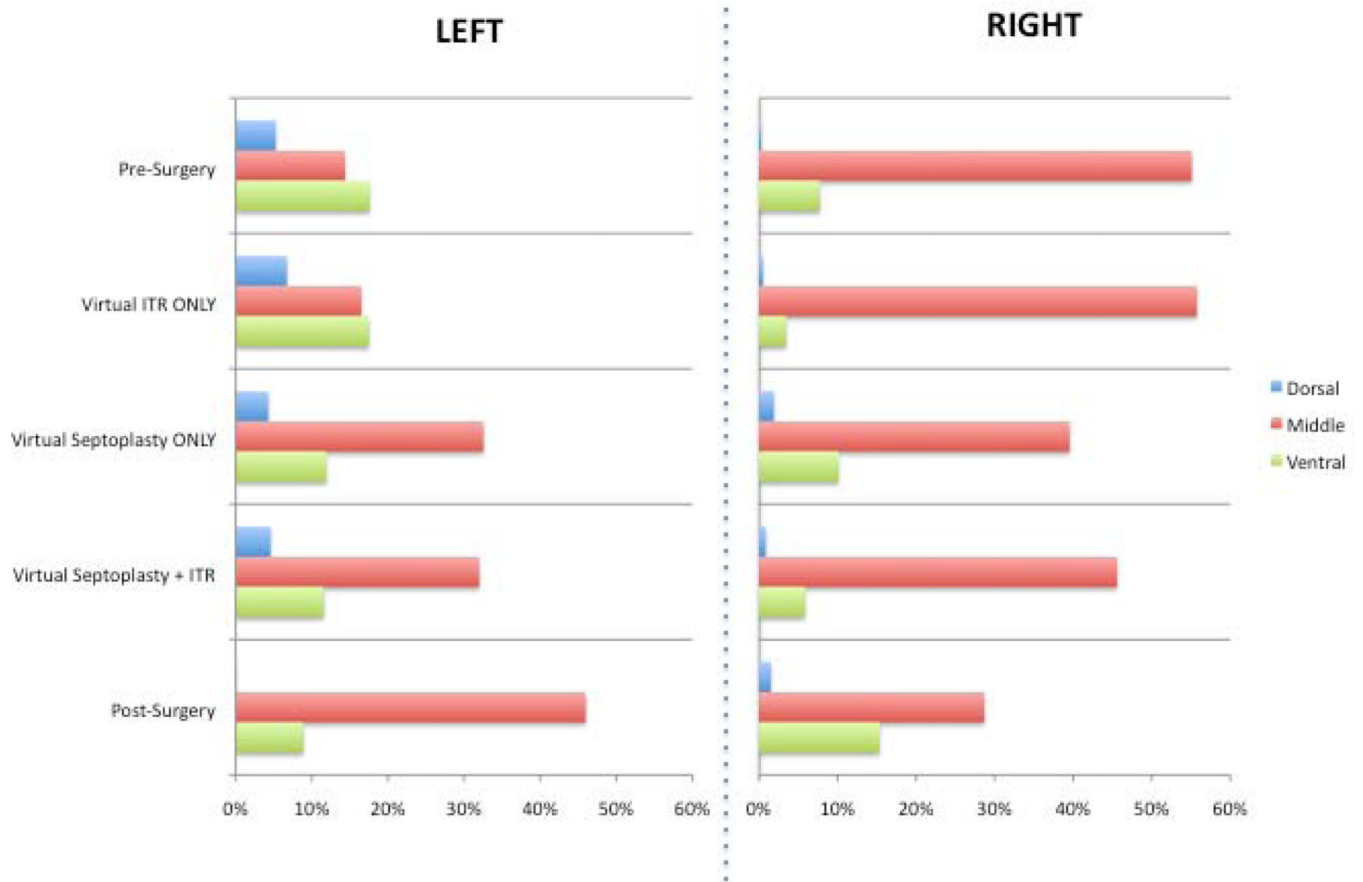


**FIGURE 6.** CFD-calculated regional airflow distribution between the dorsal, middle, and ventral regions of the nose on the left and right sides.